

MARTIN MARIETTA

ORNL/CSD/TM-228

Particle Size Distributions Formed by Atmospheric Hydrolysis of Uranium Hexafluoride

C. K. Bayne
W. D. Bostick

**ORNL INFORMATION DIVISION
TECHNICAL LIBRARY**

Report Collection

Building 9711-1, Y-12

LOAN COPY ONLY

Do NOT transfer this document to any other person. If you want others to see it, attach their names, return the document, and the Library will arrange the loan as requested.

UCN-1624 (3 3-83)

ChemRisk Document No. 1222

Y
MARIETTA ENERGY SYSTEMS, INC.
UNITED STATES
T OF ENERGY

Printed in the United States of America. Available from
National Technical Information Service
U.S. Department of Commerce
5285 Port Royal Road, Springfield, Virginia 22161
NTIS price codes—Printed Copy: A04; Microfiche A01

This report was prepared as an account of work sponsored by an agency of the United States Government. Neither the United States Government nor any agency thereof, nor any of their employees, makes any warranty, express or implied, or assumes any legal liability or responsibility for the accuracy, completeness, or usefulness of any information, apparatus, product, or process disclosed, or represents that its use would not infringe privately owned rights. Reference herein to any specific commercial product, process, or service by trade name, trademark, manufacturer, or otherwise, does not necessarily constitute or imply its endorsement, recommendation, or favoring by the United States Government or any agency thereof. The views and opinions of authors expressed herein do not necessarily state or reflect those of the United States Government or any agency thereof.

Internal Correspondence

MARTIN MARIETTA ENERGY SYSTEMS, INC.


February 28, 1985

To: Recipients of Subject Report

Report No: ORNL/CSD/TM-228 Classification: Unclassified
Authors: C. K. Bayne and W. D. Bostick
Subject: "Particle Size Distributions Formed by Atmospheric Hydrolysis
of Uranium Hexafluoride"

The report number ORNL/CSD/TM-9387 that appears on the cover, title page and distribution page of this report is in error. Please correct by placing the enclosed self-adhesive pages on your copy(ies) of this report.

We regret any inconvenience this error may have caused and appreciate your cooperation in correcting it.


W. N. Drewery, Supervisor
Laboratory Records Department
Information Resources Organization

WND:ddb

cc: Master File ORNL/CSD/TM-228-RC

PARTICLE SIZE DISTRIBUTIONS FORMED BY ATMOSPHERIC HYDROLYSIS
OF URANIUM HEXAFLUORIDE

C. K. Bayne

Computing and Telecommunications Division
at Oak Ridge National Laboratory
P. O. Box X
Oak Ridge, Tennessee 37831

W. D. Bostick

Materials and Chemistry Technology Department
at Oak Ridge Gaseous Diffusion Plant
Oak Ridge, Tennessee 37831

Date Published: January 1985

Martin Marietta Energy Systems, Inc.
Operating the
Oak Ridge National Laboratory . Oak Ridge Y-12 Plant
Oak Ridge Gaseous Diffusion Plant . Paducah Gaseous Diffusion Plant
under Contract No. DE-AC05-84OR21400
for the
DEPARTMENT OF ENERGY

2 Plant
ous Diffusion Plant



3 4456 0041647 7

Figure 1. The effect of the concentration of the *Agaricus bisporus* spores on the growth of *Agaricus bisporus* on the substrate.

CONTENTS

TABLE OF FIGURES	v
TABLE OF TABLES.vii
ACKNOWLEDGMENTS.	ix
ABSTRACT	1
I. INTRODUCTION	1
II. PARTICLE SIZE DATA.	3
III. PROBABILITY DISTRIBUTION ANALYSIS.	7
IV. APPLICATION TO UO_2F_2 GEOMETRIC PARTICLE SIZE NUMBER DISTRIBUTION	21
V. CONCLUSION	29
REFERENCES	31
APPENDIX A	33

TABLE OF FIGURES

1. Capture Efficiency for 4g/cm^3 Particles in a Multistage Cascade Impactor.	4
2. Kurtosis versus $B1 = (\text{Skewness})^2$ for Pickrell's Data on Atmospheric Hydrolysis of Uranium Hexafluoride.	9
3. Cumulative Distributions for the Best (Table 1) and Worst (Table 4) Fits of Johnson's S_B Curve.	14
4. Johnson's S_B Theoretical Probability Density Functions.	15
5. Johnson's S_B Theoretical Probability Density Functions.	16
6. Johnson's S_B Theoretical Probability Density Functions.	17
7. Johnson's S_B Theoretical Probability Density Functions.	18
8. Johnson's S_B Theoretical Probability Density Functions.	19
9. Quadratic Fit of Median Values as a Function of Release Times for the five Data Tables.	20
10. Johnson's S_B Curves Fitted to Lux's Data.	23
11. Lognormal Distributions Fitted to Lux's Data.	24
12. Lognormal Distribution for Number and Mass Frequencies of Lux's Data.	26
13. Kurtosis versus $B1 = (\text{Skewness})^2$ for Pickrell's Table 1 Data for both Mass and Number Frequencies	28

TABLE OF TABLES

1.	Particle sizes (micrometers) at 0%, 50%, and 100% capture probabilities for cascade impactor stages	3
2.	Relative humidity, release temperature, and time after release from Pickrell (1982).	5
3.	Estimated G and H parameters for Johnson's system	12
4.	Values of B1 and B2 for Lux's data	21
5.	Parameter estimates for Johnson's S_B and lognormal distribution with their sum of squares (SS)	22
A.1.	Mass fractions (Pickrell, 1982) at 50% particle size diameters (micrometers) for the five data tables at different sampling times	34
A.2.	Frequency of the number of particle sizes mass fractions (Lux, 1982) for static (FS), dynamic (FD), and catastrophic (FC) release modes.	36

ACKNOWLEDGMENTS

The authors acknowledge with appreciation the helpful comments provided by Max D. Morris, from Engineering Physics and Mathematics Division, and P. W. Pickrell, from Process Support Division. The authors express their appreciation also to Joyce Poland, of Computing and Telecommunications Division, for typing the manuscript.

Funds for the support of this work were provided by the Department of Energy.

PARTICLE SIZE DISTRIBUTIONS FORMED BY ATMOSPHERIC HYDROLYSIS
OF URANIUM HEXAFLUORIDE

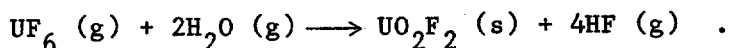
C. K. Bayne and W. D. Bostick

ABSTRACT

The probability model for particle size data is usually assumed to be lognormal. For Pickrell's (1982) UF_6 data, the lognormal is inappropriate and Johnson's S_B frequency curves are shown to be suitable alternative models. The type of particle size measurement, either mass or number, is also an important consideration for modeling. Converting from one measurement type to the other illustrated by UF_6 aerosol data does not necessarily preserve the same probability distribution.

I. INTRODUCTION

When gaseous uranium hexafluoride (UF_6) is released into the atmosphere, it rapidly reacts with ambient moisture to form an aerosol of uranyl fluoride (UO_2F_2) particles and hydrogen fluoride (HF) vapor:



The U.S. Department of Energy has mandated a safety analysis effort to evaluate the potential for accident and to predict the human health consequences of postulated UF_6 releases. Evaluation of the aerodynamic behavior of aerosol particulates is an important component in this effort, because this property is a major determinant in the settling rate (and, hence, the dispersion) of the uranium-containing material (Bostick et al., 1984).

Pickrell (1982) has summarized the results (Appendix A1) for a number of experimental releases of UF_6 in a contained volume under a variety of static conditions, including the relative humidity of the air and the temperature of the UF_6 at the instant of its release. For a series of experiments, aerodynamic particle size distributions were obtained as a function of time elapsed from the moment of release. Our objective in this communication is to present a detailed statistical evaluation of the particle size data presented by Pickrell.

In particular, we sought to derive a probability distribution function to adequately describe the experimental data obtained at any given sampling interval, and secondarily, to relate distributional parameters to the experimental variables of elapsed time, humidity, and pre-release temperature of the UF_6 sample. This information is expected to be of value to DOE sponsored investigators developing dispersion models for transport of uranyl fluoride particulates under postulated release conditions.

The probability distribution of particle sizes is usually examined by histograms, or an assumed lognormal distribution is fitted to the data. Other distributional forms have been suggested by Sehmel (1968) and Viswanathan and Mani (1982). The present analysis uses skewness and kurtosis statistics derived from the data to first determine the form of the probability distribution. These forms are then selected from Johnson's system of frequency curves (Johnson, 1949). Parameters used to determine the shape of these empirical distributions have not yet been demonstrated to correlate with the experimental variables of relative humidity and release temperature.

II. PARTICLE SIZE DATA

A piezoelectric quartz-crystal microbalance impactor (model PC-2, California Measurements, Inc.) was used to measure mass concentration and particle size distribution of air suspended UF_6 particles. The aerosol stream entering the 10-stage cascade impactor encounters the largest nozzle first, with nozzles becoming progressively smaller in the subsequent stages. Each stage collects particles in a defined range of diameter sizes. It is customary to designate a stage by the particle size at which there is a 50% probability of capture of a specific mass density. Table 1 gives the 0%, 50%, and 100% capture probabilities for the UF_6 experiment. These probabilities were calculated from capture probabilities given in Fig. 1 derived from the instruction manual for the piezoelectric QCM cascade impactor by assuming a particle density of 4g/cm^3 (Bostick et al., 1984).

Table 1. Particle sizes (micrometers) at 0%, 50%, and 100% capture probabilities for cascade impactor stages.

Stage	0%	50%	100%
1	12.021	17.678	26.163
2	6.010	8.839	12.021
3	3.005	4.526	6.010
4	1.520	2.263	3.005
5	0.778	1.131	1.520
6	0.375	0.566	0.778
7	0.219	0.283	0.375
8	0.106	0.141	0.219
9	0.050	0.071	0.106
10	0.023	0.035	0.050

Associated with each stage is a mass concentration that represents a fraction of the total mass captured in that stage. These mass fractions can also be interpreted as mass probabilities of particle sizes in a given

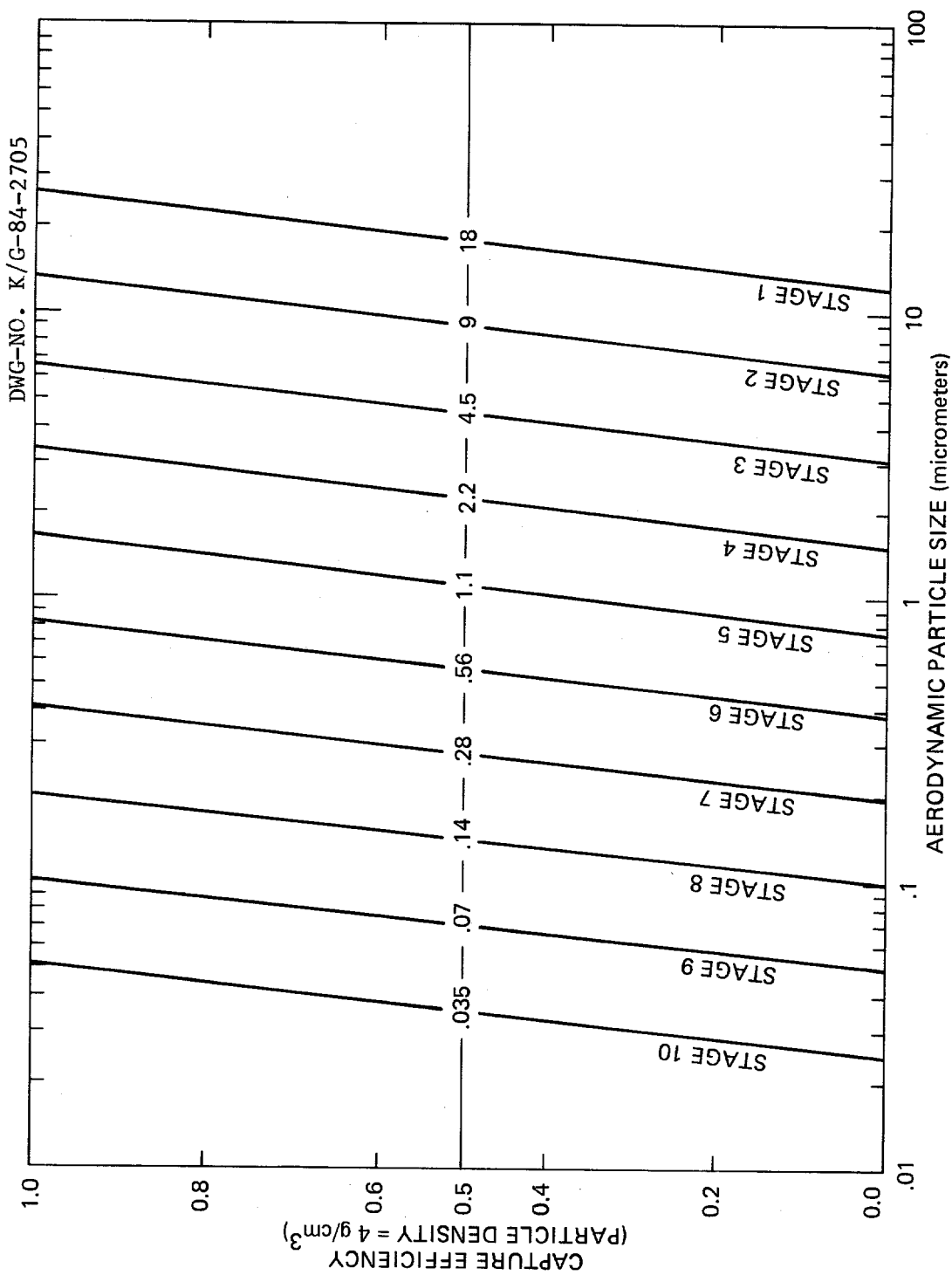


Fig. 1. Capture Efficiency for 4 g/cm^3 Particles in a Multistage Cascade Impactor (Adapted from Instruction Manual, QCM Model PC-2, California Measurements, Inc.).

stage. Mass fractions for the UF_6 experiments are recorded in five tables by Pickrell (1982), see Table A.1. These five tables represent different relative humidity, release temperatures, and sampling times. Table 2 shows 31 different conditions under which aerosols were collected.

Table 2. Relative humidity, release temperature, and time after release from Pickrell (1982). Table entries are the data table numbers (i.e., 1, 2, 3, 4, and 5).

Humidity:	33%	85%	70%	70%	100%
Temp. :	65 °C	65-69 °C	75 °C	100 °C	85 °C
Time					
3				4	
4					5
8	1	2	3		
17	1				
18					5
20			3		
25				4	
30					5
38	1				
40			3		
45					5
52		2			
55				4	
90		2	3		5
120				4	
150		2			5
180	1			4	
210		2			
300			3		
330		2			5
360	1			4	
390			3		
420		2			

Table 2 shows that experimental conditions varied a great deal. Relative humidity and release temperature effects were not properly controlled as a factorial design and thus the two effects are statistically partially confounded. This confounding of the effects may explain the difficulty of relating distributional parameters to these two factors. In addition, elapsed time before sampling was not taken at uniform intervals and this factor is also confounded with the other two factors.

III. PROBABILITY DISTRIBUTION ANALYSIS

Particle size probability models can be based on four moments calculated from the data. Suppose for fixed values of the three experimental factors (i.e., relative humidity, release temperature, and sampling time), the 50% diameter is denoted by D_j for the j -th stage and denote the corresponding mass fraction by f_j , then the mean of the data is calculated by:

$$\bar{D} = \sum_{j=1}^{10} D_j f_j .$$

The second, third, and fourth central moments can then be calculated by:

$$M_k = \sum_{j=1}^{10} (D_j - \bar{D})^k f_j, \quad k = 2, 3, 4 .$$

The skewness and kurtosis statistics based on the standardized third and fourth central moments, respectively, can be used to determine many distributions.

$$\sqrt{B1} = \text{skewness} = M_3 / (M_2)^{3/2}$$

$$B2 = \text{kurtosis} = M_4 / (M_2)^2 .$$

A distribution that is symmetrical will have theoretical skewness of zero. A distribution with a long tail extending to the right will usually have a positive skewness while those extending to the left will usually have a negative skewness. Kurtosis is sometimes interpreted as the peakedness of the distribution. However, kurtosis values are very much dependent on the shape of distributional tails and may have little to do with any central peak. The theoretical skewness and kurtosis values of the normal

distribution are $(\sqrt{\beta_1}, \beta_2) = (0, 3)$. Other distributions can be determined either by $(\sqrt{\beta_1}, \beta_2)$ or a function of $(\sqrt{\beta_1}, \beta_2)$. For example, the lognormal distribution is determined by the parametric form:

$$\beta_1 = (w-1)(w+2)^2$$

$$\beta_2 = w^4 + 2w^3 + 3w^2 - 3$$

where $w = \exp(\text{variance of } \ln(\text{data}))$.

For the data summarized in Table A.1, Fig. 2 is a plot of sample kurtosis values versus B_1 values (squared sample skewness values). Theoretical values for the lognormal distribution are superimposed on the graph. These results show that the lognormal distribution is not a very good probability model for these particle size distributions. Also the (B_1, B_2) values fall on a line defined by:

$$B_2 = 2.65 + 1.05B_1$$

even though the data were collected under a variety of conditions. This result indicates that all of the particle size distributions are in the same general class of distribution.

A method of empirically modeling the distribution is to transform the data so that it has a normal distribution. The Johnson's system (Johnson, 1949) of distributions is a method of transforming data to have a normal distribution. This system has three types of transformations: 1) S_U systems for data with an unbounded range $-\infty < D < +\infty$, 2) S_L system for lognormal data with a semi-bounded range $0 < D < +\infty$, and 3) S_B system for data with a bounded range $A < D < B$. In Fig. 2, the S_L system is represented by the β_2 vs β_1 curve for lognormal data and is the boundary

ORNL-DWG84-16937

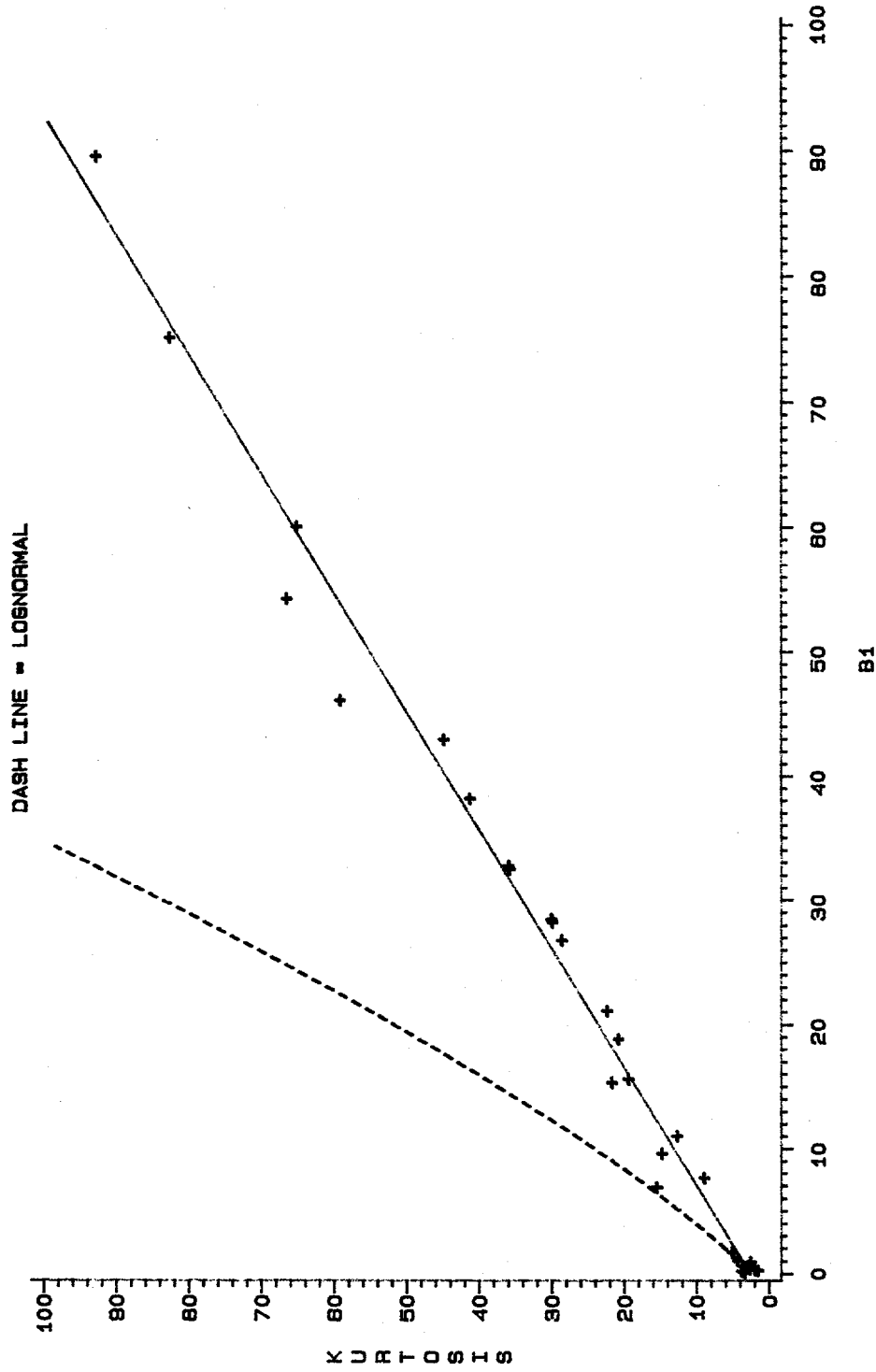


Fig. 2. Kurtosis versus $B1 = (\text{Skewness})^2$ for Pickrell's Data on Atmospheric Hydrolysis of Uranium Hexafluoride.

between S_U and S_B . B2 values above the lognormal curve are in S_U and values below the lognormal curve are in S_B . The B2 versus B1 plot in Fig. 2 indicates that the particle size data fall into the S_B system. This implies that the following transformation for particle sizes in the range $A < D < B$ should be used.

$$Y = (D-A)/(B-A), \quad 0 < Y < 1,$$

$$Z = G + H \ln(Y/(1-Y))$$

where Z is a standardized normal variate (i.e., zero mean, and variance equal to one). To fit particle size distributions with this transformation, the four parameters A , B , G , and H must be estimated from the data.

The two parameters A , and B representing the endpoints of the particle size range were assigned the values:

$$A = 0.01, \text{ and}$$

$$B = 27.0$$

These values were chosen by considering the possible upper and lower limits of the data range (see Table 1 and Fig. 1).

Parameters G and H are estimated by fitting theoretical probability values to data frequency values. Let f_j correspond to a mass frequency value for particle size D_j in the interval $a_j < D_j < b_j$. This means that

$$\Pr(a_j < D_j < b_j) = f_j$$

The theoretical probability density function, $p(D)$ in Johnson's S_B system is:

$$p(D) = H \cdot \exp(-0.5 \cdot Z^2) / [\sqrt{(2 \cdot \pi)} \cdot (B-A) \cdot Y \cdot (1-Y)]$$

with $\pi = 3.14159 \dots$

To calculate the theoretical value corresponding to f_j , the density function, $p(D)$, is integrated over the interval $a_j < D_j < b_j$. Call this theoretical probability $P_j(G, H)$ to denote the dependency on the parameters G and H . Parameters G and H are estimated by minimizing the following sum of squares for a fixed set of data conditions (i.e., relative humidity, release temperature, and sampling time):

$$SS = \text{Sum of Squares} = \sum_{j=1}^{10} (f_j - P_j(G, H))^2$$

This minimization was done by using PROC NLIN in the Statistical Analysis System (SAS, 1982). Estimated values for G and H are tabulated in Table 3. These estimates can be used to calculate a theoretical particle size frequency for any of the 10 impactor stages. For example, the G and H estimates in data Table 1 for 8 minutes are $G = 14.44$ and $H = 3.09$. The theoretical particle size frequency for stage 7 is:

$$0.219 < D < 0.375$$

$$0.0077 < Y = (D - 0.01) / (27.0 - 0.01) < 0.0135$$

$$-0.5737 < Z = 14.44 + 3.09 \ln(Y / (1 - Y)) < 1.1793$$

$$\Pr(-0.5737 < Z < 1.1793) = Q(1.1793) - Q(-0.5737)$$

$$\Pr(-0.5737 < Z < 1.1793) = 0.88 - 0.28 = 0.60$$

where for the standardized normal variate Z : $Q(z) = \Pr(-\infty < Z < z)$. The observed frequency for this stage is $f_7 = 0.55$.

Table 3. Estimated G and H parameters for Johnson's S_B system. Included are the minimum sum of square values, standard deviations of the estimates and median values of the theoretical distributions.

Table	Time	G	H	St Dev G	St Dev H	Sum of Squares	Median
1	8	14.44	3.09	1.27	0.26	0.0135	0.260
1	17	8.25	1.85	0.44	0.10	0.0036	0.321
1	38	6.90	1.61	0.86	0.19	0.0198	0.379
1	180	4.71	1.18	0.42	0.10	0.0097	0.508
1	360	5.88	1.45	0.31	0.07	0.0039	0.469
2	8	12.86	2.97	1.70	0.40	0.0127	0.359
2	52	10.15	2.56	1.45	0.35	0.0455	0.514
2	90	6.35	1.47	1.26	0.28	0.0472	0.363
2	150	6.40	1.50	1.36	0.31	0.0576	0.389
2	210	5.30	1.24	0.83	0.19	0.0277	0.383
2	330	7.01	1.68	0.89	0.20	0.0226	0.413
2	420	4.14	0.88	0.73	0.15	0.0278	0.255
3	0	15.29	3.32	1.63	0.35	0.0291	0.279
3	20	12.94	2.82	1.60	0.35	0.0368	0.283
3	40	9.27	2.04	1.55	0.34	0.0414	0.293
3	90	3.29	0.69	0.77	0.15	0.0380	0.230
3	300	3.25	0.58	0.95	0.18	0.0536	0.113
3	390	3.39	0.60	0.89	0.16	0.0442	0.103
4	3	14.05	3.03	2.33	0.49	0.0588	0.269
4	25	7.71	1.82	1.05	0.24	0.0249	0.395
4	55	5.75	1.42	0.87	0.21	0.0319	0.476
4	120	8.96	2.71	1.52	0.43	0.0408	0.960
4	180	7.89	2.39	1.57	0.45	0.0655	0.967
4	360	3.41	0.73	0.56	0.11	0.0201	0.264
5	4	5.46	1.18	0.96	0.20	0.0333	0.271
5	18	4.86	1.04	0.83	0.17	0.0293	0.258
5	30	5.62	1.33	1.28	0.29	0.0624	0.401
5	45	5.67	1.38	0.99	0.23	0.0401	0.447
5	90	3.81	0.93	0.82	0.19	0.0435	0.467
5	150	4.45	1.12	0.86	0.21	0.0426	0.505
5	330	4.07	0.96	0.83	0.19	0.0391	0.387

Goodness of fit is judged by examining plots of the fitted probability values. Figure 3 plots the cumulative distribution function (i.e., $\Pr(0 < D < \text{diameter})$) for the best case (Table 1, sample time = 180) with $SS = 0.0036$ and worst case (Table 5, sample time = 150) with $SS = 0.0655$. Most of the fitted probability distributions fell somewhere in between these two cases with an overall average of $SS = 0.0344$. Some difficulties encountered with fitting distributional functions are due to the bimodality and large frequency at smaller diameters for some data sets. Except for five or six cases, most fits were judged to be relatively good for this data. Using estimated G and H values, theoretical probability density functions for particle sizes can be drawn and are illustrated in Figs. 4-8.

In Fig. 9, the computed median aerodynamic particle size is plotted as a function of time elapsed from the moment of UF_6 release. This figure confirms the qualitative observation (Pickrell, 1982) that initially after the release, the average particle size tends to increase, due to the process of particle agglomeration. After a relatively longer time, average airborne particle size decreases, due to the more rapid sedimentation of the larger agglomerates (Bostick et al., 1984). An attempt was also made to correlate the parameters in Table 3 with the experimental conditions of humidity and release temperature. However, no conclusion inference could be made from this study.

TABLE 1 (17 MIN) & TABLE 4 (180 MIN)

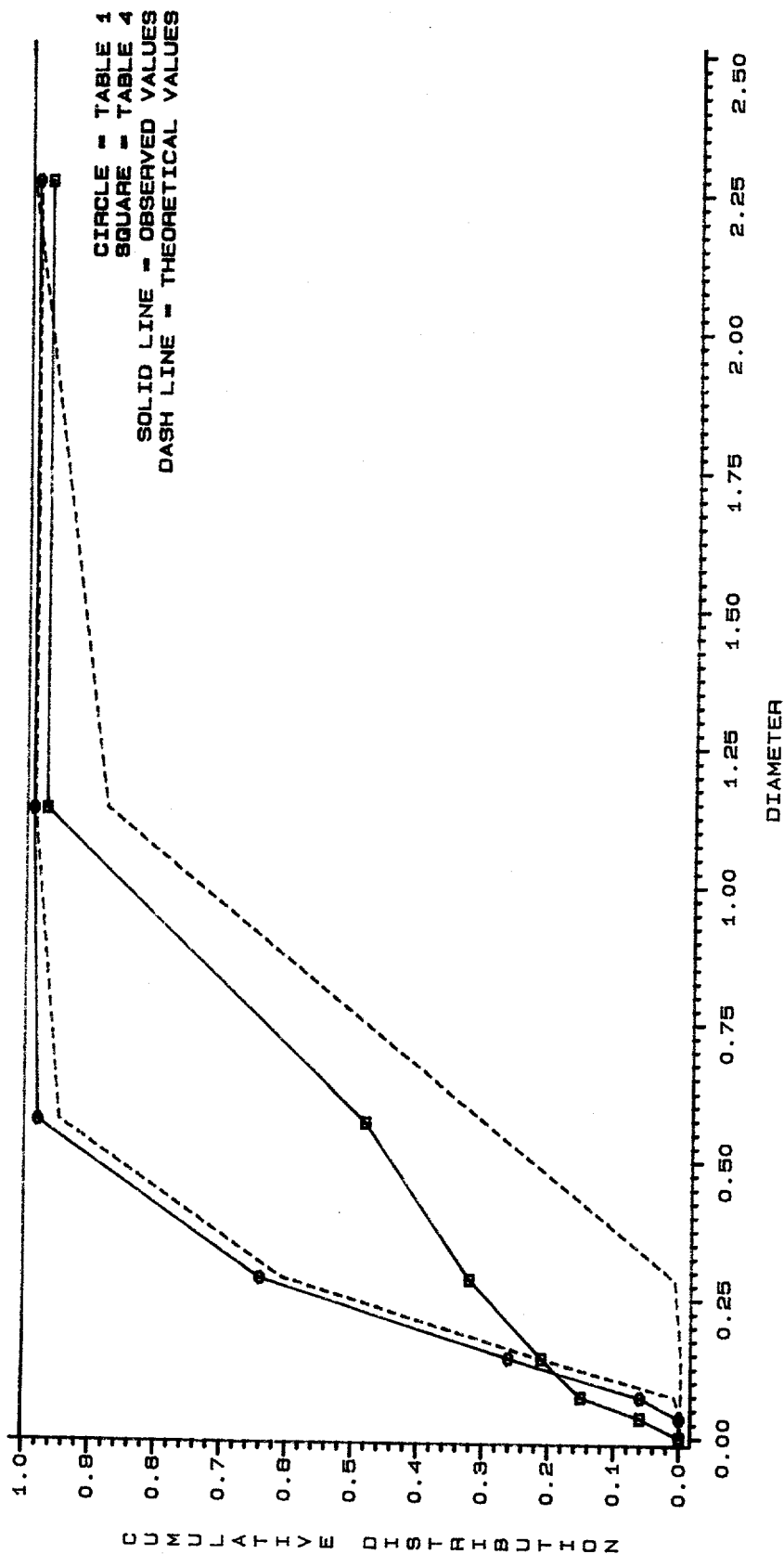


Fig. 3. Cumulative Distributions for the Best (Table 1) and Worst (Table 4) Fits of Johnson's S_B Curve.

TABLE I 35% RH

ORNL-DWG84-16939

A = 8 MIN
 B = 17 MIN
 C = 36 MIN
 D = 180 MIN
 E = 360 MIN

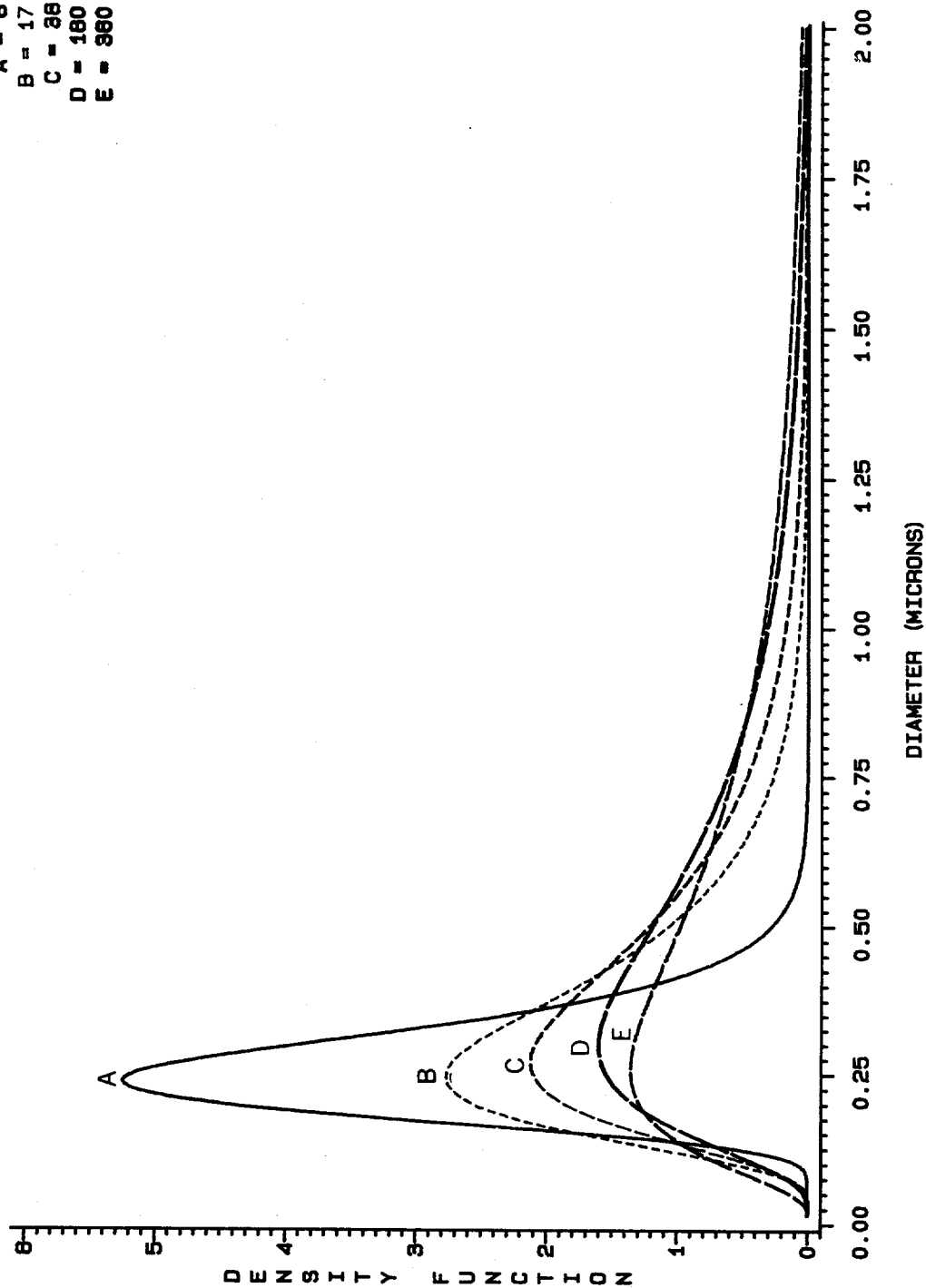
Fig. 4. Johnson's S_B Theoretical Probability Density Functions.

TABLE II 85% RH

ORNL-DWG84-16940

A = 8 MIN
B = 52 MIN
C = 80 MIN
D = 150 MIN
E = 210 MIN
F = 330 MIN
G = 420 MIN

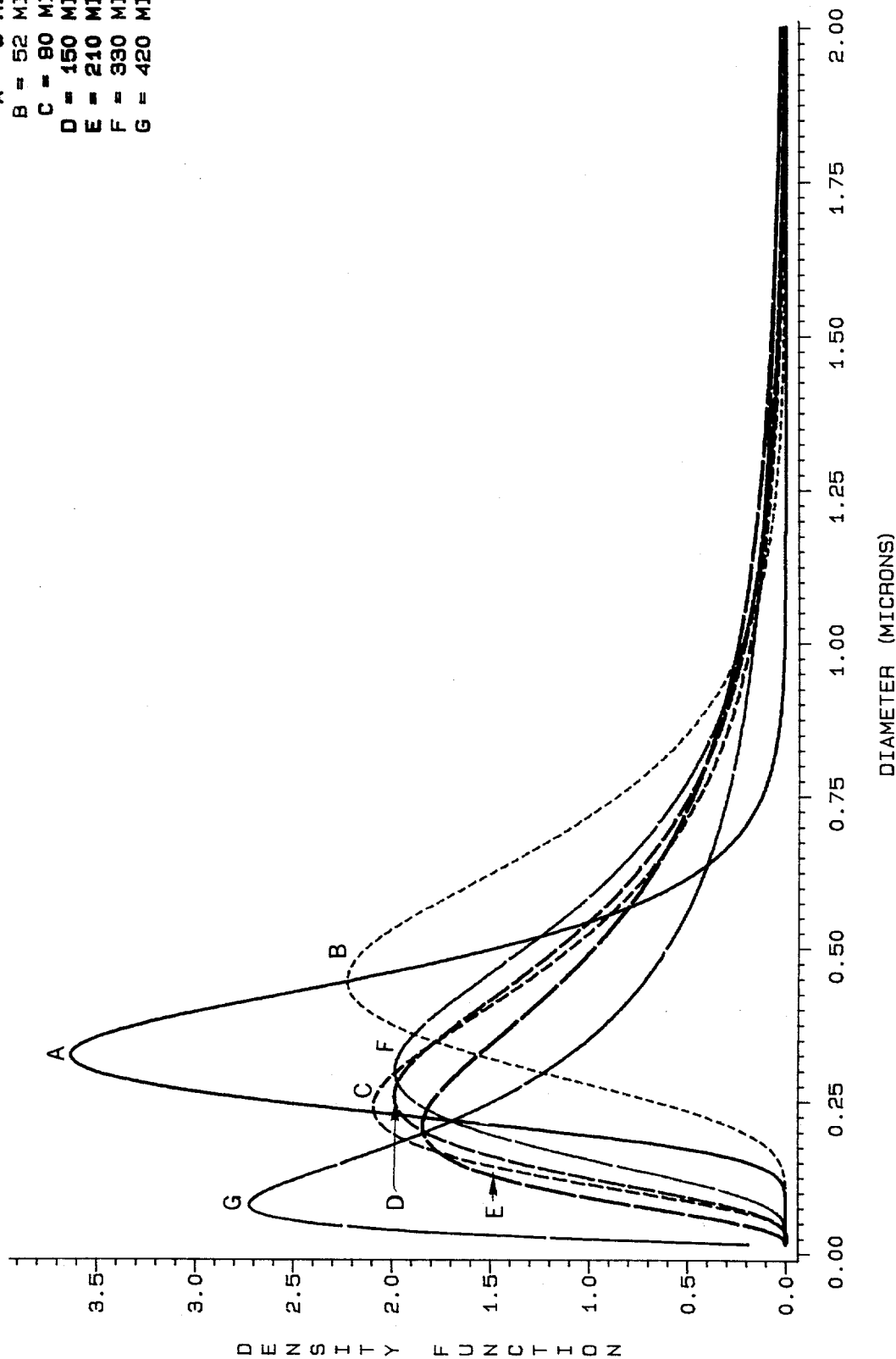


Fig. 5. Johnson's S_B Theoretical Probability Density Function.

TABLE III 70% RH

ORNL-DWG84-16941

A = 6 MIN
 B = 20 MIN
 C = 40 MIN
 D = 80 MIN
 E = 300 MIN
 F = 390 MIN

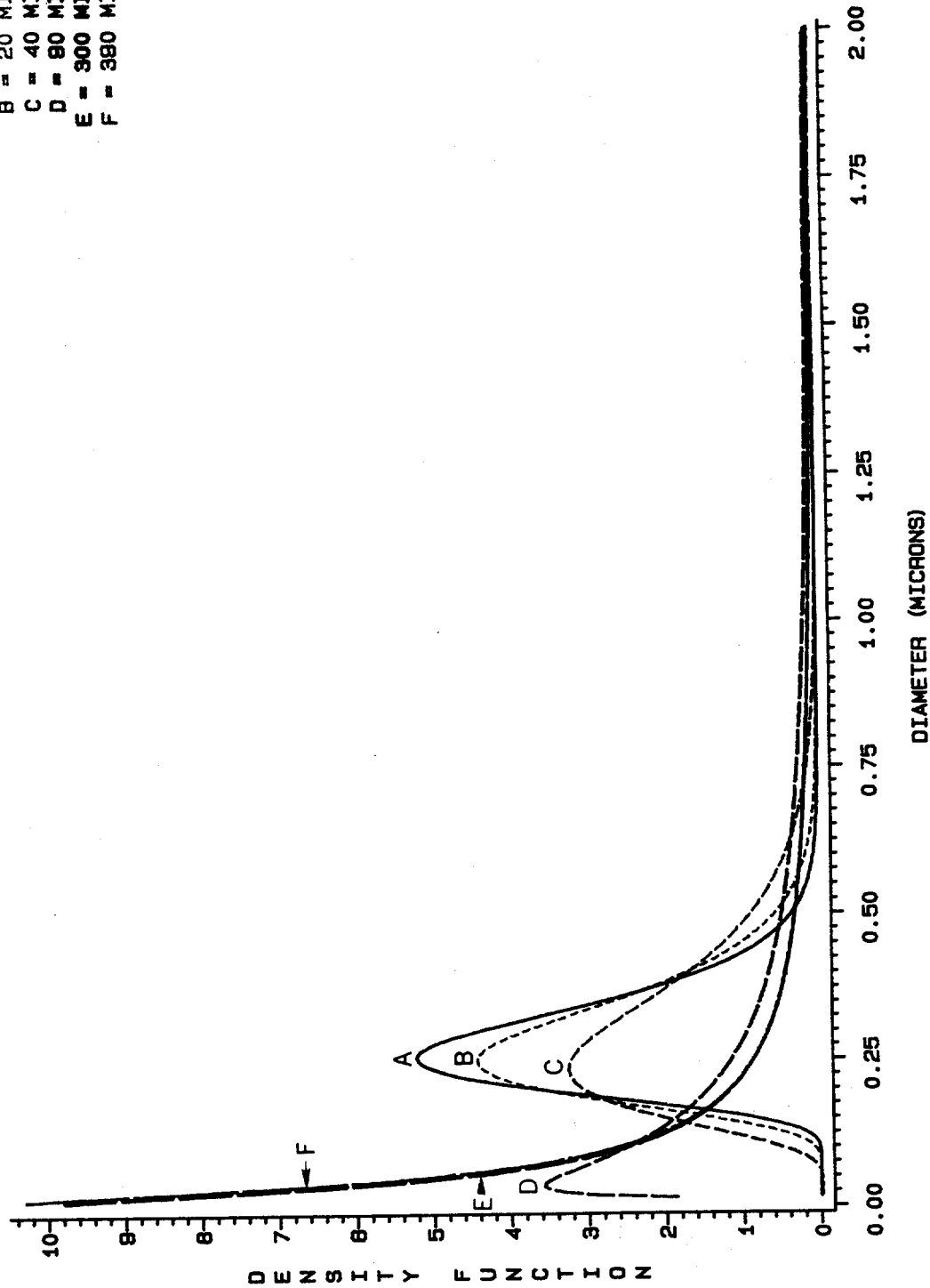
Fig. 6. Johnson's S_B Theoretical Probability Density Functions.

TABLE IV 70% RH

ORNL-DWG84-16942

A = 3 MIN
 B = 25 MIN
 C = 55 MIN
 D = 120 MIN
 E = 180 MIN
 F = 360 MIN

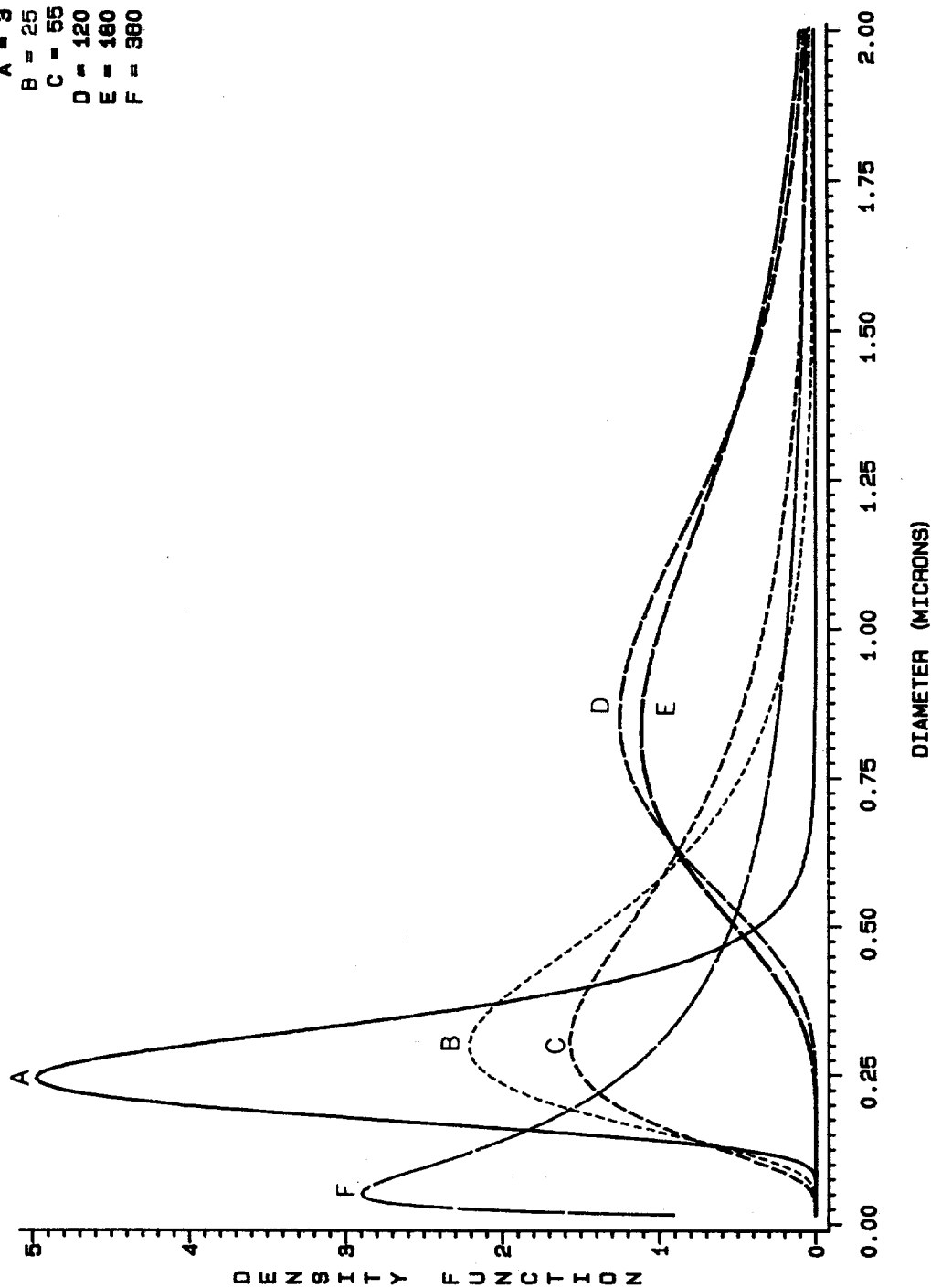
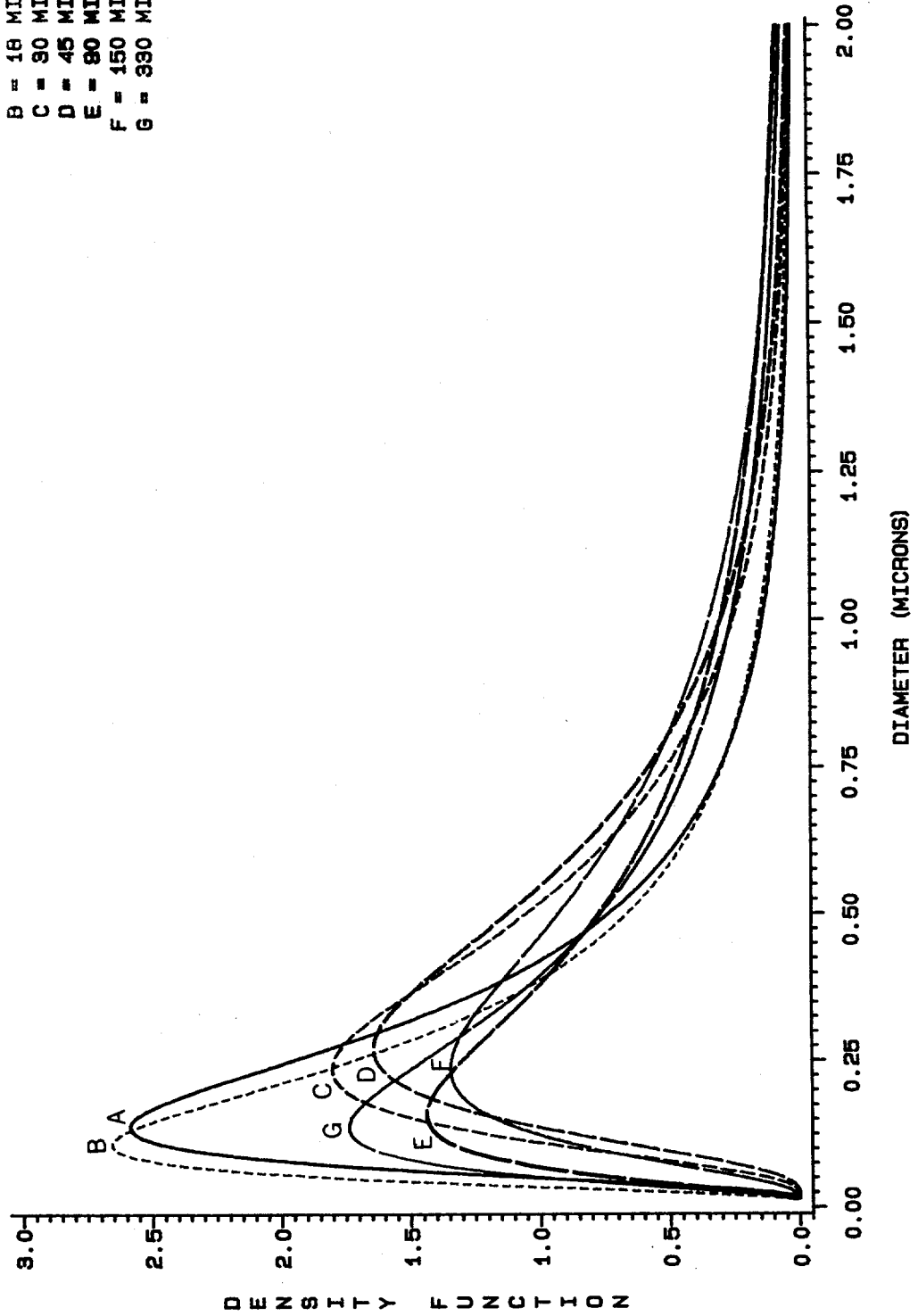


Fig. 7. Johnson's S_B Theoretical Probability Density Functions.

TABLE V 100% RH

ORNL-DWG84-16943

A = 4 MIN
 B = 18 MIN
 C = 30 MIN
 D = 45 MIN
 E = 80 MIN
 F = 150 MIN
 G = 330 MIN

Fig. 8. Johnson's S_B Theoretical Probability Density Functions.

MEDIAN

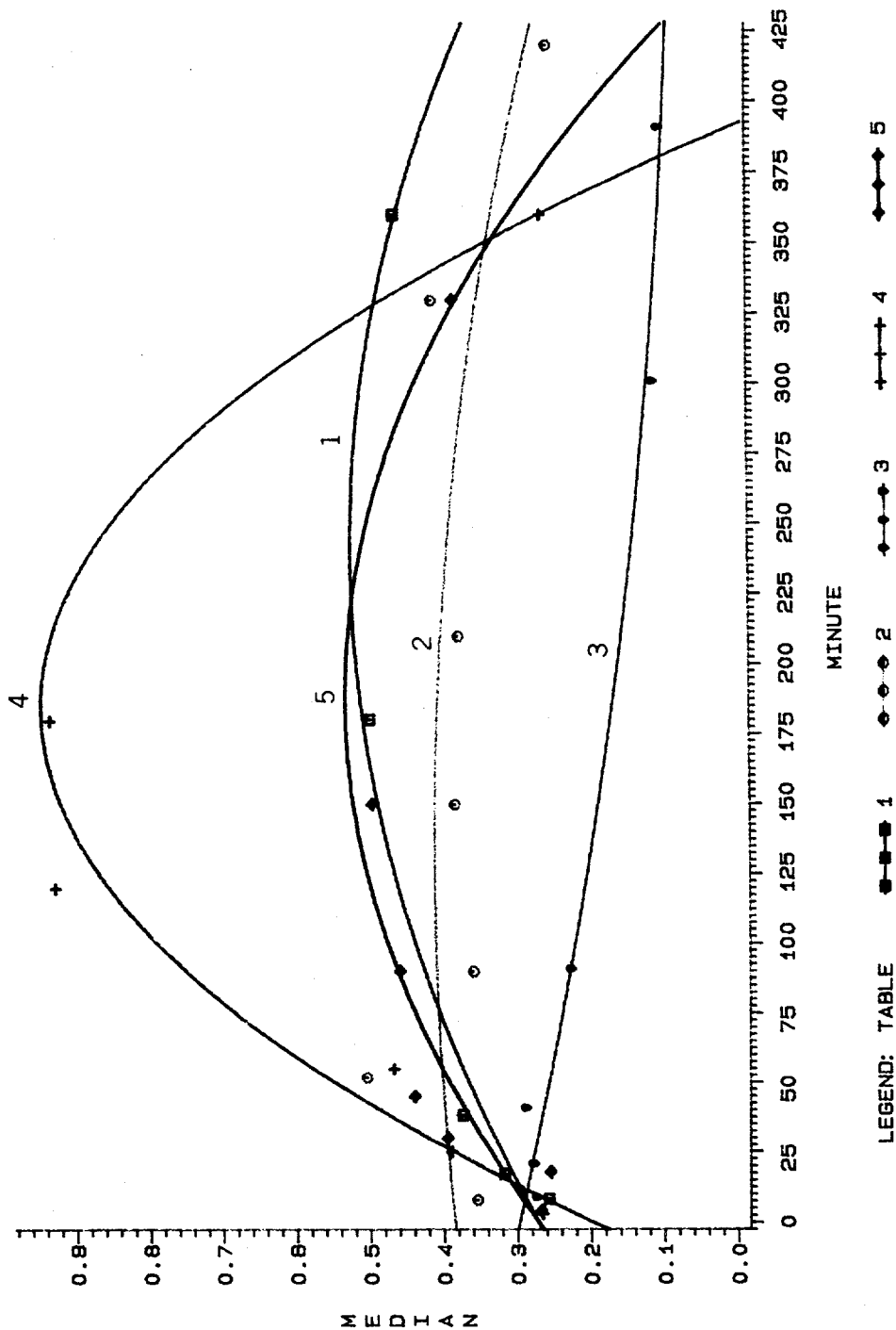


Fig. 9. Quadratic Fit of Median Values as a Function of Release Times for the five Data Tables.

IV. APPLICATION TO UO_2F_2 GEOMETRIC PARTICLE SIZE NUMBER DISTRIBUTION

Lux (1982) has reported on the measurement of the geometric particle size number distribution in the fallout material from a series of experimental UF_6 releases. Lux makes the qualitative observation that relative humidity (20% to 90% RH), ambient air temperature (0 to 40°C), and sample size do not seriously affect the UO_2F_2 particulate size distribution (0.5 to 3.0 μ). Results (Appendix A2) were tabulated for pooled data (i.e., varying conditions of RH and air temperature) under three experimental release conditions. These conditions are designated as "static", "dynamic", and simulated "catastrophic" conditions. These designations refer to the release mode:

1. Static is a release in stagnant air.
2. Dynamic is a release into a simulated 2 to 4.5 mph cross-wind.
3. Catastrophic is a rapid release and evaporation of liquid UF_6 .

Lux's data is analyzed using the methods in the previous section.

Table 4 shows the B1 and B2 values for the three release modes.

Table 4. Values of B1 and B2 for Lux's data.

Data	B1	B2
Static	3.45	7.37
Dynamic	3.94	7.58
Catastrophic	0.27	3.81

These B1 and B2 values are close to the lognormal curve and suggest that either a lognormal or S_B distribution may fit the data equally well. To fit the lognormal distribution, the following transformation can be used:

$$Z = G + H \ln(D), \quad 0 < D < \infty$$

where Z is a standardized normal variate. The statistic for the fitted Johnson's S_B and lognormal distributions are given in Table 5.

Table 5. Parameter estimates for Johnson's S_B and lognormal distributions with their sum of squares (SS). The standard deviations of the estimates are in parentheses.

Data	Johnson S_B				Lognormal			
	SS	G	H	Median	SS	G	H	Median
Static	0.0027	3.07 (0.17)	1.71 (0.09)	1.44	0.0030	-0.72 (0.08)	2.04 (0.11)	1.42
Dynamic	0.0011	2.95 (0.11)	1.55 (0.05)	1.30	0.0014	-0.46 (0.05)	1.80 (0.07)	1.29
Catastrophic	0.0041	4.46 (0.28)	1.79 (0.10)	0.77	0.0049	0.50 (0.09)	1.94 (0.12)	0.77

Both distributions fit the data very well with Johnson's S_B distribution having a slightly smaller sum of squares than the lognormal sum of squares. The density function for the two fits are plotted in Figs. 10 and 11. Inferences are the same from either distribution. The median particle size decreases with the severity of the release mode with catastrophic mode being the largest decrease.

It is important to bear in mind that Lux's data represent a number distribution for uranyl fluoride particles in fallout material, sorted by geometric particle size. Whereas, Pickrell's data represent mass distribution for airborne material, sorted by aerodynamic particle size. Number and mass distributions can be related if the simplifying assumption is made that particles are spherical:

LUX DATA

JOHNSON SB-CURVES

ORNL-DWG84-16945

A - STATIC
B - DYNAMIC
C - CATASTROPHIC

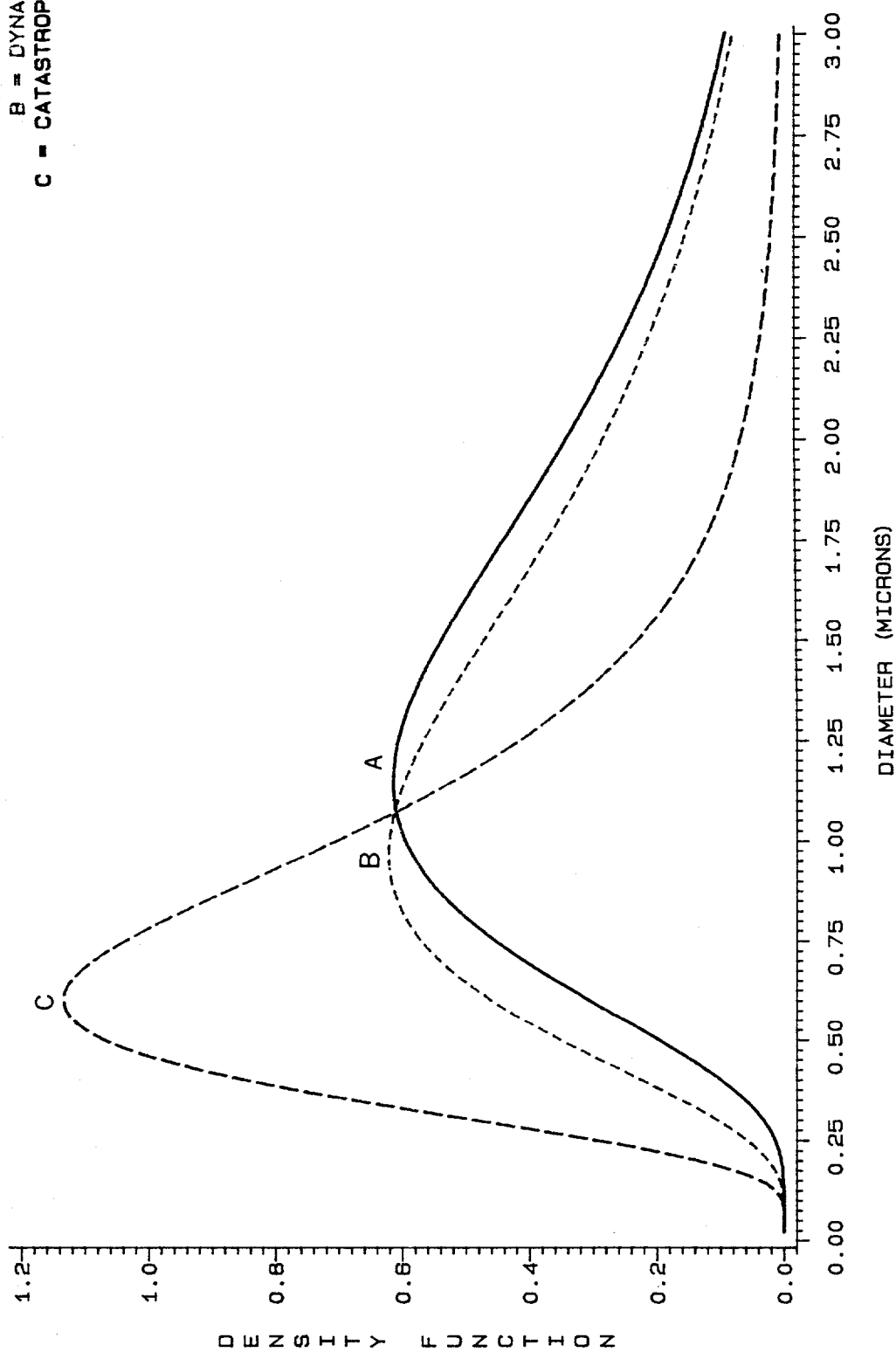


Fig. 10. Johnson's S_B Curves Fitted to Lux's Data.

LUX DATA LOGNORMAL CURVES

ORNL-DWG84-16946

A = STATIC
B = DYNAMIC
C = CATASTROPHIC

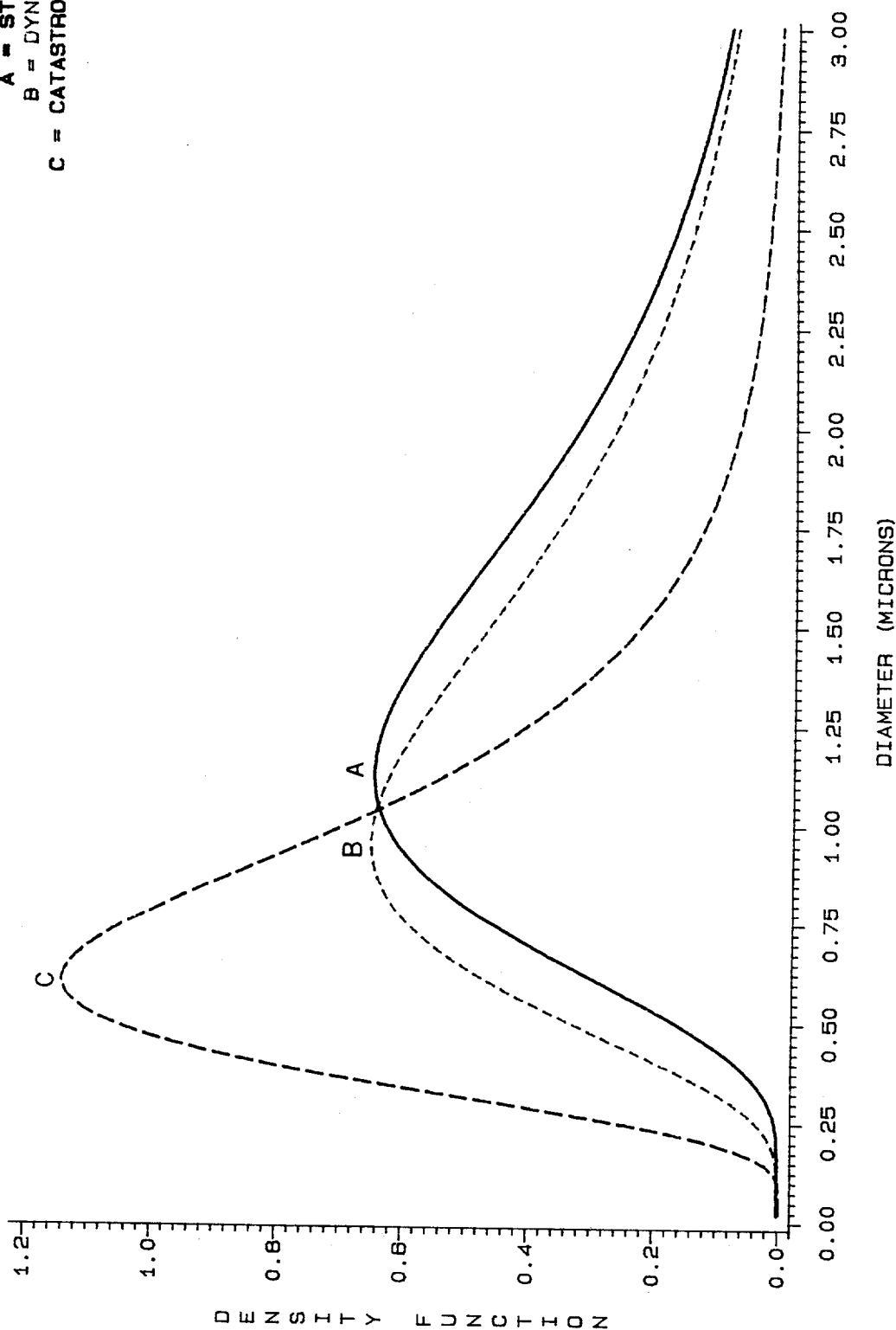


Fig. 11. Lognormal Distributions Fitted to Lux's Data.

N = Total number of particles.

M = Total mass particles

g_j = Number frequency for the j -th interval.

f_j = Mass frequency for the j -th interval.

d = Particle density.

For the j -th interval, $j = 1, 2, \dots, 10$, we have:

Mass = Number x volume x density

$$Mf_j = (Ng_j)(\pi D_j^3/6)d.$$

Because the mass frequencies sum to one, we have the relation:

$$f_j = g_j D_j^3 / \sum g_j D_j^3, \quad j = 1, 2, \dots, 10.$$

Using this relationship, Lux's data were converted to mass frequency.

The 50% diameters were used for the first nine intervals while the diameter for the tenth interval was calculated as an average diameter over the last interval assuming a lognormal distribution of the particle numbers. This modification reduced the diameter size used for the last interval. Reducing the diameter for the tenth interval was done to minimize the effect of the arbitrary assignment of 50% diameters to the last interval. Because diameters are cubed, the diameter for the last interval makes a major contribution to mass frequencies.

Converted mass frequency distributions were then fitted using both lognormal and Johnson's frequency distributions. The lognormal distributions are displayed in Fig. 12 and show a shift to the right with the median value about twice that for number frequencies. Both lognormal and Johnson's frequency distributions adequately describe the mass

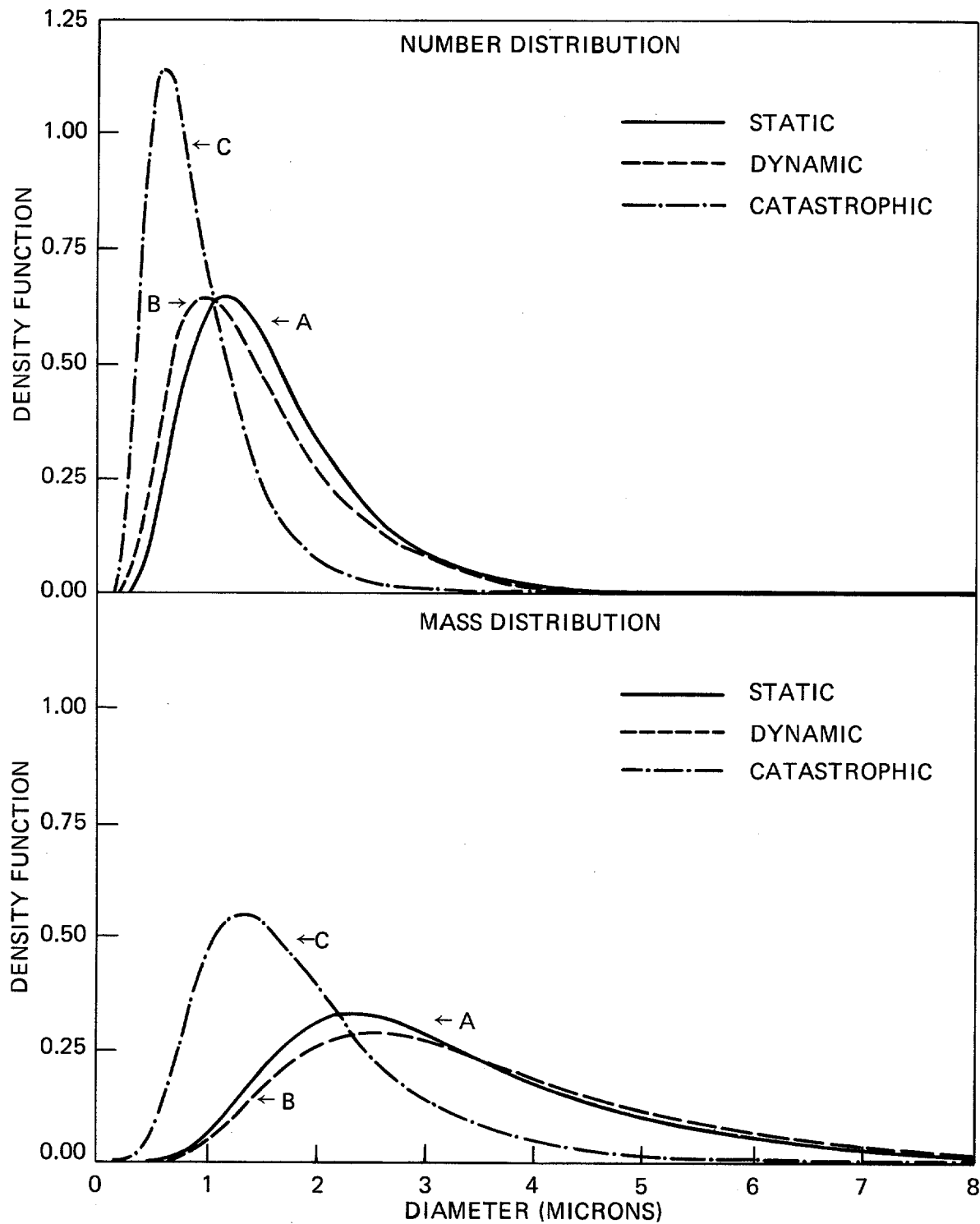


Fig. 12. Lognormal Distribution for Number and Mass Frequencies of Lux's Data.

frequency distribution. For Lux's data, the lognormal distribution is preserved under the conversion of number to mass frequencies.

The conversion of mass frequency to number frequency can also be made. The effect of this conversion was examined by calculating changes in the skewness and kurtosis statistics. Pickrell's Table 1 data was used because the mass frequencies are distributed as Johnson's frequencies and are not lognormal. The number frequency for the j -th interval was calculated by:

$$g_j = (f_j/D_j^3) / \sum (f_j/D_j^3) \text{ for } j = 1, 2, \dots, 10$$

These conversions used mass frequencies and 50% diameters in Table A.1 and no modifications of any diameters were made.

Calculated $B_1 = (\text{skewness})^2$ and kurtosis values are plotted in Fig. 13. These plots show that the number frequency would be better approximated by a lognormal distribution than Johnson's frequency distributions. This study implies that the distribution that approximates mass frequency may not apply to number frequency.

PICKRELL

TABLE 1 DATA

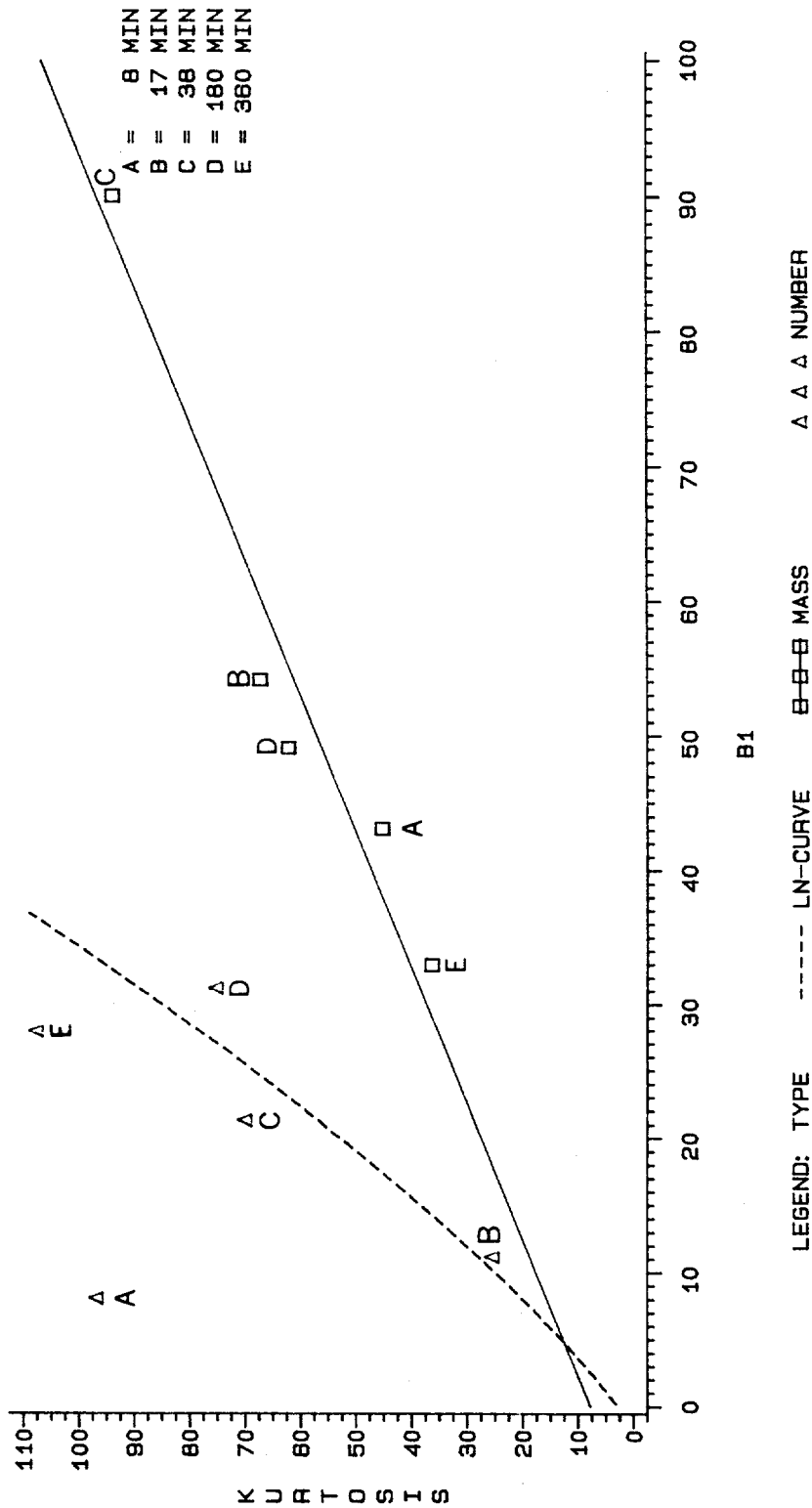


Fig. 13. Kurtosis versus $B1 = (\text{Skewness})^2$ for Pickrell's Table 1 Data for both Mass and Number Frequencies.

IV. CONCLUSIONS

This study demonstrated that lognormal is not always a good assumption for the distribution of particle size data collected on UF_6 aerosols. The Johnson's S_B system is introduced as a method of fitting the particle size data. This system transforms the data so it can be approximated by the standardized normal distribution. Reasonable fits were judged to occur in most cases. Correlation of distributional properties with experimental conditions are inconclusive.

The type of frequencies, either mass or number, is also an important consideration for modeling. Number frequencies appear to be adequately approximated by lognormal distributions and mass frequencies appear to be adequately approximated by Johnson's frequency distributions. However, converting from number to mass or from mass to number frequencies does not necessarily preserve the distributional type.

Future experiments should consider doing factorial experiments using different levels of relative humidity and release temperatures. Factorial experiments would permit independent estimates of the two effects. During the experiment, sampling times should be taken in uniform increments for all combinations of relative humidity and release times.

REFERENCES

1. W. D. Bostick, W. H. McCulla, and P. W. Pickrell, "Sampling, Characterization, and Remote Sensing of Aerosols Formed in the Atmospheric Hydrolysis of Uranium Hexafluoride", K/PS-5042, Oak Ridge Gaseous Diffusion Plant, Oak Ridge, TN, 1984.
2. P. W. Pickrell, "Characterization of the Solid, Airborne Materials Created by the Interaction of UF_6 with Atmospheric Moisture in a Contained Volume", UCC-ND Report K/PS-144, Oak Ridge Gaseous Diffusion Plant, Oak Ridge, TN, 1982.
3. G. A. Sehmel, "A Particle Size Distribution Function for Data Recorded in Size Ranges", Ann. Occup. Hyg., 11, pp. 87-89, (1968).
4. K. Viswanathan and B. P. Mani, "A New particle Size Distribution", Ind. Eng. Chem. Process Des. Dev., 21, pp. 776-78, (1982).
5. N. L. Johnson, "System of Frequency Curves Generated by Methods of Translation", Biometrika, 36, pp. 149-76, (1949).
6. Instruction Manual, "Piezoelectric QCM Cascade Impactor Model PC-2", California Measurement, Inc., Sierra Madre, CA 91024, 1980.
7. SAS Institute, Inc., "SAS User's Guide: Statistics", Cary, NC, 1982.
8. C. J. Lux, "Evaluation of Techniques for Controlling UF_6 Release Clouds in the GAT Environment Chamber", AT-T-3116, Goodyear Atomic Corporation, Piketon, OH, 1982.

APPENDIX A
Experimental Data

Table A.1. Mass Fractions (Pickrell, 1982) at 50% particle size diameters (micrometers) for the five data tables at different sampling times.

Data from Table 1, 35% R.H.

OBS	DIAM	F8	F17	F38	F180	F360
1	17.678	0.02	0.00	0.01	0.00	0.02
2	8.839	0.00	0.00	0.00	0.01	0.01
3	4.526	0.01	0.01	0.00	0.00	0.01
4	2.263	0.00	0.00	0.01	0.02	0.01
5	1.131	0.02	0.01	0.02	0.26	0.17
6	0.566	0.07	0.34	0.44	0.35	0.42
7	0.283	0.55	0.38	0.24	0.16	0.20
8	0.141	0.24	0.20	0.18	0.17	0.13
9	0.071	0.08	0.06	0.08	0.03	0.02
10	0.035	0.00	0.00	0.01	0.01	0.01

Data from Table 2, 85% R.H.

OBS	DIAM	F8	F52	F90	F150	F210	F330	F420
1	17.678	0.00	0.00	0.00	0.00	0.04	0.03	0.03
2	8.839	0.00	0.00	0.00	0.00	0.00	0.00	0.00
3	4.526	0.00	0.00	0.00	0.03	0.00	0.00	0.00
4	2.263	0.00	0.00	0.01	0.02	0.02	0.03	0.03
5	1.131	0.01	0.05	0.03	0.05	0.10	0.08	0.07
6	0.566	0.40	0.60	0.33	0.32	0.29	0.39	0.17
7	0.283	0.46	0.10	0.29	0.29	0.29	0.28	0.31
8	0.141	0.02	0.05	0.08	0.03	0.08	0.05	0.16
9	0.071	0.09	0.15	0.16	0.15	0.10	0.08	0.12
10	0.035	0.02	0.05	0.10	0.11	0.08	0.08	0.11

Table A.1. (cont'd)

Data from Table 3, 70% R.H.

OBS	DIAM	F8	F20	F40	F90	F300	F390
1	17.678	0.05	0.00	0.08	0.02	0.00	0.03
2	8.839	0.04	0.00	0.02	0.00	0.00	0.00
3	4.526	0.00	0.04	0.03	0.02	0.00	0.02
4	2.263	0.02	0.00	0.00	0.01	0.02	0.00
5	1.131	0.00	0.02	0.05	0.08	0.05	0.03
6	0.566	0.08	0.12	0.17	0.18	0.12	0.10
7	0.283	0.58	0.50	0.39	0.28	0.30	0.28
8	0.141	0.13	0.14	0.14	0.14	0.16	0.16
9	0.071	0.10	0.10	0.07	0.08	0.11	0.12
10	0.035	0.00	0.08	0.05	0.18	0.27	0.26

Data from Table 4, 70% R.H. Repeat.

OBS	DIAM	F3	F25	F55	F120	F180	F360
1	17.678	0.00	0.01	0.00	0.00	0.03	0.00
2	8.839	0.00	0.01	0.00	0.00	0.00	0.00
3	4.526	0.01	0.00	0.02	0.00	0.00	0.00
4	2.263	0.00	0.00	0.02	0.00	0.00	0.00
5	1.131	0.00	0.02	0.12	0.55	0.49	0.17
6	0.566	0.06	0.43	0.43	0.18	0.16	0.21
7	0.283	0.52	0.27	0.14	0.08	0.11	0.21
8	0.141	0.17	0.10	0.10	0.05	0.06	0.12
9	0.071	0.19	0.12	0.13	0.08	0.09	0.20
10	0.035	0.05	0.04	0.04	0.05	0.06	0.09

Table A.1. (cont'd)

Data from Table 5, 100% R.H.

OBS	DIAM	F4	F18	F30	F45	F90	F150	F330
1	17.678	0.00	0.00	0.00	0.00	0.00	0.02	0.00
2	8.839	0.00	0.00	0.00	0.00	0.00	0.01	0.00
3	4.526	0.00	0.00	0.00	0.00	0.00	0.01	0.00
4	2.263	0.00	0.00	0.00	0.00	0.00	0.00	0.00
5	1.131	0.01	0.03	0.04	0.11	0.22	0.19	0.13
6	0.566	0.24	0.24	0.40	0.40	0.31	0.33	0.34
7	0.283	0.34	0.32	0.18	0.18	0.14	0.15	0.18
8	0.141	0.16	0.16	0.09	0.08	0.06	0.04	0.08
9	0.071	0.17	0.18	0.18	0.16	0.16	0.15	0.16
10	0.035	0.07	0.08	0.11	0.08	0.11	0.10	0.11

Table A.2. Frequency of the number of particle sizes mass fractions (Lux, 1982) for static (FS), dynamic (FD), and catastrophic (FC) release modes.

OBS	0% DIAM	50% DIAM	100% DIAM	FS	FD	FC
1	0.01	0.25	0.50	0.0162	0.0412	0.2193
2	0.50	0.65	0.80	0.0970	0.1588	0.2973
3	0.80	0.95	1.10	0.1745	0.1735	0.2797
4	1.10	1.25	1.40	0.2004	0.1824	0.1286
5	1.40	1.60	1.80	0.1616	0.1529	0.0526
6	1.80	1.95	2.10	0.1081	0.0980	0.0107
7	2.10	2.25	2.40	0.0905	0.0735	0.0117
8	2.40	2.55	2.70	0.0582	0.0471	0.0000
9	2.70	2.85	3.00	0.0517	0.0235	0.0000
10	3.00	5.00	7.00	0.0420	0.0500	0.0000

INTERNAL DISTRIBUTION

- | | |
|--|---------------------------------|
| 1-5. C. K. Bayne | 29. M. D. Morris |
| 6-10. W. D. Bostick | 30. T. A. Nolan |
| 11. K. O. Bowman | 31. J. A. Parsons |
| 12. J. R. Bradbury | 32. P. W. Pickrell |
| 13. W. J. Crowley | 33. D. H. Pike |
| 14. J. Dykstra | 34. R. C. Riepe |
| 15. J. L. Gambel | 35. F. O. Sternberg |
| 16. W. R. Golliher | 36. L. D. Trowbridge |
| 17. R. W. Holmberg | 37. G. W. Westley |
| 18-23. R. A. Just | 38-39. Central Research Library |
| 24. J. M. Kennerly | 40. Document Reference |
| 25. G. J. Kidd | Section Y-12 |
| 26. R. P. Leinius/G. E. Whitesides/
CTD Library | 41-42. Laboratory Records |
| 27. W. H. McCulla | 43. Laboratory Records - RC |
| 28. J. R. Merriman | 44. ORNL Patent Office |
| | 45. ORGDP Library |

EXTERNAL DISTRIBUTION

46. J. N. Rogers, Div. 8474. Sandia National Laboratories, Livermore, CA 94550.
47. Office of Assistant Manager for Energy Research and Development, Department of Energy, Oak Ridge Operations, Oak Ridge, TN 37830.
48. Division of Engineering, Mathematics and Geosciences, Department of Energy, Washington, D.C. 20545
49. C. E. Creek, 103 Essex Lane, Oak Ridge, TN 37830
50. V. S. Emler, Goodyear Atomic Corporation, P. O. Box 628, Piketon, OH 45661.
51. C. J. Lux, Goodyear Atomic Corporation, P. O. Box 628, Piketon, OH 45661.
52. D. W. Sheffey, DOE/ORO, Federal Building, Oak Ridge, TN 37830.
- 53-79. Technical Information Center, Oak Ridge, TN 37830.